Supplementary Material

Highly efficient and stable ZnO-based perovskite solar cells enabled by a self-assembled monolayer as the interface linker

Yan Wu[a,b], Jiaxing Song[*b], Xianrui Wu[b], Chufeng Qiu[b], Xinxing Yin[b], Lin Hu[b], Zhen Su[b], Yingzhi Jin[b], Jianjun Chen[a], Zaifang Li[*b]

[a] Institute of Advanced Ceramic Material & Fiber, School of Materials Science and Engineering, Zhejiang Sci-Tech University, Hangzhou 310018, PR China

[b] China-Australia Institute for Advanced Materials and Manufacturing, Jiaxing University, Jiaxing 314001, PR China

Experimental

Materials

Zinc acetate dehydrate ($Zn(CH_3COO)_2 \cdot 2H_2O$, 98%), ethanolamine (>99%), 2-methoxyethanol anhydrous (99.8%), Chlorobenzene (CB, 99.8%), N, N-Dimethylformamide (DMF, 99.8%) were purchased from Sigma-Aldrich. 2-Thiopheneacetic acid (2-TA, 98%), 3-Thiopheneacetic acid (3-TA, 98%), Dimethyl sulfoxide (DMSO, 99.7%) and acetonitrile anhydrous (ACN, 99%) were purchased from Energy Chemical. Formamidine Hydroiodide (FAI, ≥99.5%), Cesium iodide (CsI, 99.9%), Lead iodide (PbI_2, >99.99%), Lead bromide ($PbBr_2$, >99.99%), Spiro-OMeTAD (2,2',7,7'-tetrakis-(N,N-di-4-methoxyphenylamino)-9,9'-spirobifluorene, >99.0%), 4-tert-butylpyridine (tBP, >99%) and lithium salts (Li-TFSI, >96%) were purchased from Xi'an Polymer Light Technology Corp. All the chemicals and solvents were kept in the glove-box before starting our experiment.

Device fabrication

All devices were prepared on the cleaned and patterned ITO substrates. All ITO glasses were cleaned with deionized water, acetone, and isopropanol in sequence by 30 min ultrasonication. After washing, the substrates were dried with a nitrogen gas flow. Before spin-coating, the ITO substrates were further treated with plasma for 10 minutes to remove organic residues. For ZnO layer, 0.734 g of zinc acetate dehydrate with 0.28 g of ethanolamine was dissolved in 10 mL 2-methoxyethanol. The resulting ZnO sol-gel solution was filtered by PTFE syringe filter (0.22 um), then the ZnO solution was spin-coated at a rate of 3500 rpm for 60s onto the ITO substrates, follow by annealing at a temperature of 200 °C for 30 min in the air. After cooling, transfer the substrates to a nitrogen-filled glove box. The different thiophene acetic acid were dissolved in CB with 0.1 mg/ml. The thiophene (TA) solution was spin-coated onto ZnO at 3500 rpm for 40 s in glove-box and annealed at 100 °C for 10 min to form TA interlayer. Then wash the substrate with 200 uL CB to remove the dissociative TA molecules. For perovskite precursor solution, a mixture of PbI_2 (340.5 mg), FAI (118.1 mg), CsI (36.5 mg), $PbBr_2$ (45.5 mg) was dissolved in 1mL mixed solution of DMF and DMSO (volume ration of DMF/DMSO is 4:1). The perovskite precursor was then spin-coated onto the substrates by a consecutive two-step spin-coating process at 1000 rpm for 10 s and 6000 rpm for 30 s, respectively, and 130 uL of CB antisolvent was dropped onto the substrate at 15s before the end. Then the wet film was annealed at 100 °C for 5 min. The spiro-OMeTAD solution was prepared by dissolving 72.3 mg of spiro-OMeTAD, 10.5 uL of tBP, and 17.5 uL of Li-TFSI (520 mg/mL in acetonitrile) into 1 mL of CB. When the perovskite film was cooled to room temperature, the solution of spiro-OMeTAD was spin coated onto perovskite at 5000 rpm for 40s to form the HTL. Finally, 85 nm Ag electrodes were deposited by thermal evaporation.

Thin film characterization

XRD patterns were obtained with a Panalytical X'Pert'3 Powder X-Ray diffractometer with a Cualpha source (λ 1. 54 Å). The top-viewed SEM images was obtained by Thermo ScientificTM Apreo scanning electron microscopy. X-ray photoemission spectroscopy (XPS) data were collected with a Thermo Scientific K-Alpha+ system. The samples were measured using an Al K Alpha source. The core level spectra were recorded using a pass

energy of 50 eV from an analysis area of 400 μm×400 μm. The measurement was carried out after washing the substrates with CB. Ultraviolet photoelectron spectroscopy (UPS) profiles were measured with a monochromatic He I light source (21.22 eV) and data were collected with a Thermo ESCALAB XI+ system. A sample bias of -5 V was applied to observe the secondary electron cutoff. The work function (W_F) can be obtained by the equation of $W_F = 21.22 - E_{cutoff}$, valence band maximum (VBM) was calculated by the formula of $E_{VB} = W_F + E_{onset}$, and the conductive band minimum (CBM) was determined by the equation of $E_{CB} = E_{VB} + E_g$. Time-resolved photoluminescence (TRPL) spectra were obtained on a PL spectrometer (Edinburgh Instruments, FLS 980), excited with a picosecond pulsed diode laser (EPL-475). A Hamamatsu C5680-04 streak camera was used for TRPL. UV-Vis-NIR spectra were obtained using a Shimadzu UV-2550 spectrophotometer.

Device characterization

The current density-voltage (*J-V*) characteristics of solar cells were measured in glove-box under 100 mW/cm^2 AM 1.5G solar irradiation (Enlitech SS-F5-3A) with a Keithley 2400 Source Meter. The *J-V* curves were measured by reverse (1.5 V to -0.5 V bias) or forward scans (-0.5 V to 1.5 V bias) at the scan rate of 50 mV/s, and all devices were obtained by masking the cells with a metal mask of 0.043 cm^2 or 0.0945 cm^2 in area. The light intensity of the solar simulator was calibrated by a standard silicon solar cell provided by PV Measurements. External quantum efficiency (EQE) spectra were taken on a QE-R3011 system. The dependence of J_{sc} on P_{light} can provide information on the bimolecular recombination occurring in the photoactive layer, which follows a power law dependence, that is, $J_{sc} \propto P_{light}^{\alpha}$. The V_{oc} varies logarithmically with P_{light} and follows the relationships of $V_{oc} \propto (nkT/q)\ln(P_{light})$. Impedance spectroscopy measurement (EIS) was carried out with an Electrochemical Workstation under dark conditions in the frequency range from 0.1 Hz to 100 MHz, and the data were analyzed by the Z-View program. In the Nyquist plots, the semicircle located at the high frequency region stands for charge transfer resistance R_{tr} while the semicircle in the low frequency region is related with carrier recombination resistance R_{rec}. For transient photocurrent measurement, the system is similar to that reported previously.[1] Devices for long-term stability measurements were stored in

ambient condition (RH: ~20%, RT) , and *J-V* characteristics were performed after a period of time.

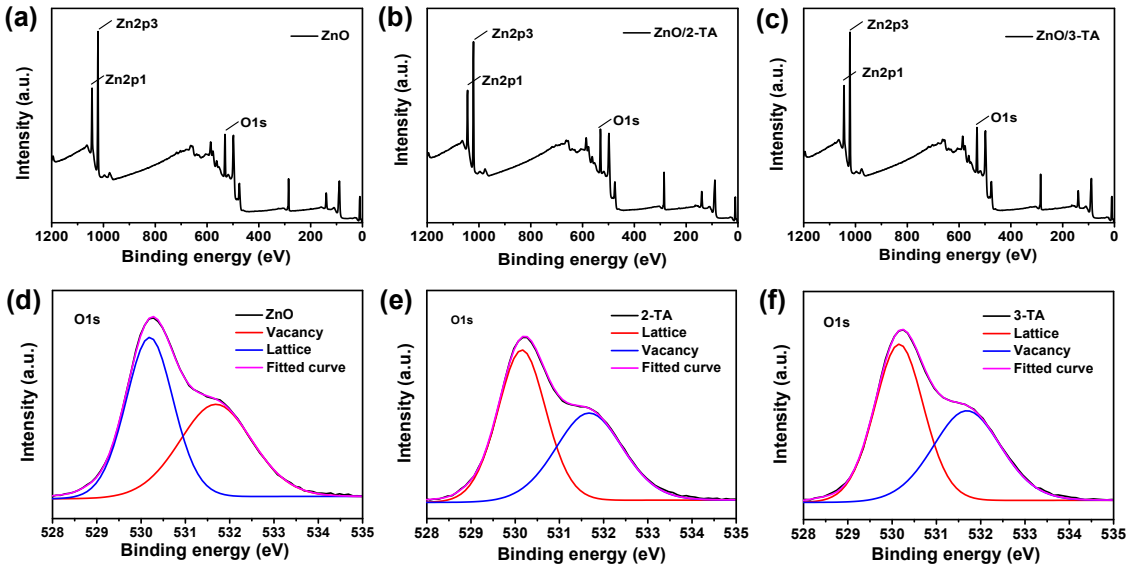

Figure S1. XPS spectra for the (a) pristine ZnO, (b) ZnO/2-TA, (c) ZnO/3-TA ETLs. O 1s core-level spectra of (d) ZnO film, (e) ZnO/2-TA film, (f) ZnO/3-TA film.

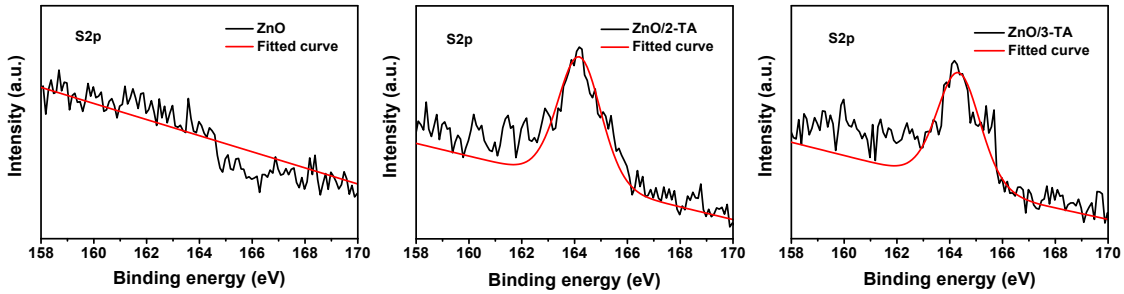

Figure S2. XPS spectra of S 2p for the pristine ZnO, ZnO/2-TA, and ZnO/3-TA ETLs.

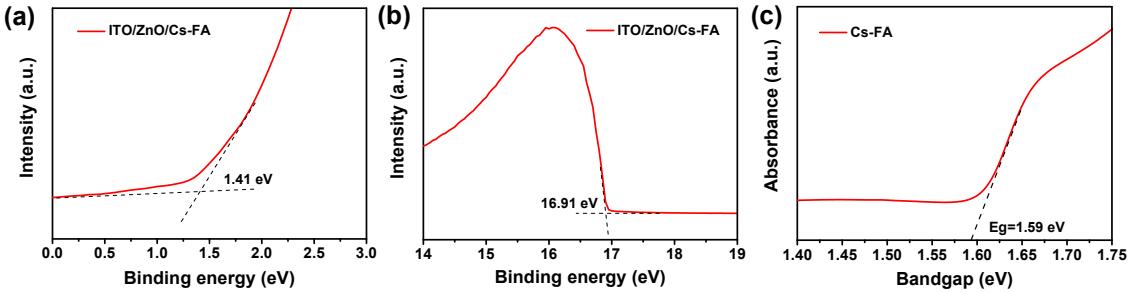

Figure S3. UPS spectra of (a) onset (b) and secondary electron cutoff of perovskite. (c) Optical bandgap of perovskite with and without SAM modification.

Table S1. The calculated energy level parameters for ZnO, ZnO/2-TA, ZnO/3-TA, and perovskite films.

	E_{onset}	E_{cutoff}	W_F	VBM	CBM
ZnO	3. 15	16. 60	4.62	7. 77	4. 55
ZnO/2-TA	3. 20	16. 81	4.41	7. 61	4. 39
ZnO/3-TA	3. 19	16. 77	4.45	7. 64	4. 42
Cs-FA	1. 41	16. 91	4.31	5. 72	4. 13

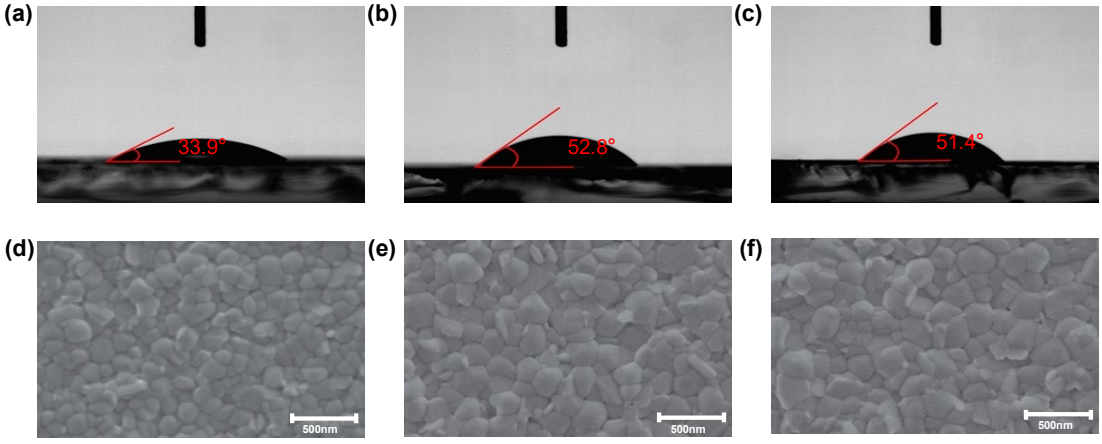

Figure S4. Water contact angles of (a) ZnO, (b) ZnO/2-TA, (c) ZnO/3-TA, and surface SEM images of perovskite films on (d) ZnO, (e) ZnO/2-TA, (f) ZnO/3-TA, respectively.

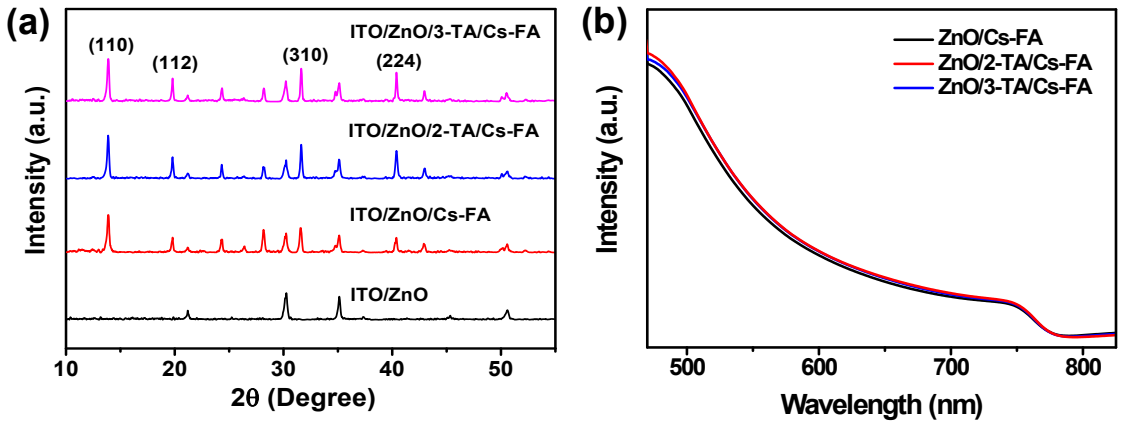

Figure S5. (a) XRD patterns and (b) UV-Vis absorption spectra of Cs-FA films grown on the different ZnO ETLs with 100 °C annealing.

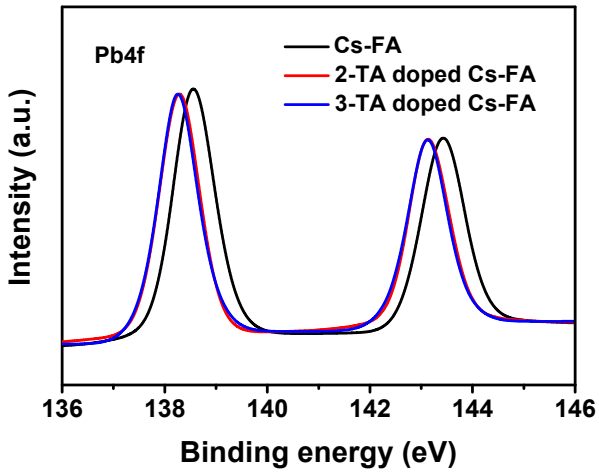

Figure S6. The Pb 4f core-level spectra for Cs-FA perovskite films.

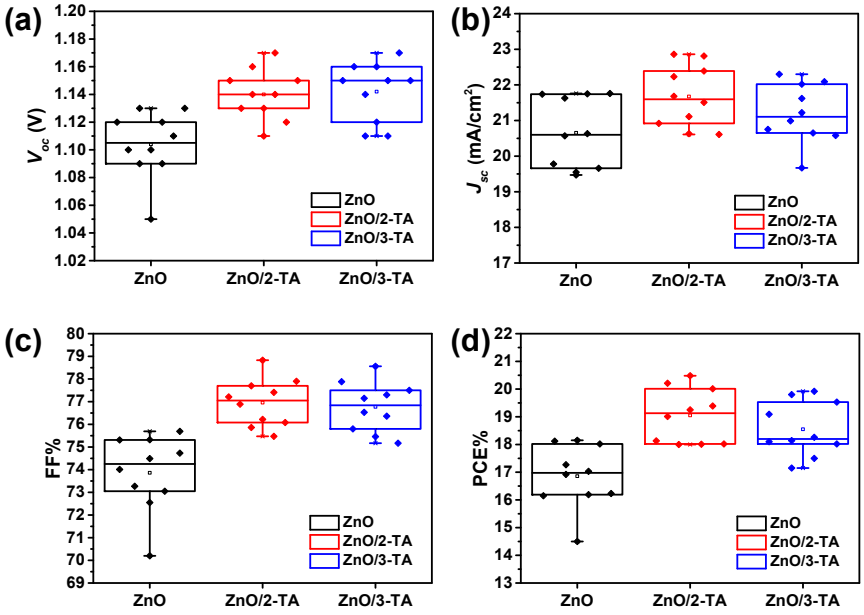

Figure S7. Statistics of photovoltaic parameters (V_{oc}, J_{sc}, FF, and PCE) for the PSC devices based on the pristine and TA-modified ZnO.

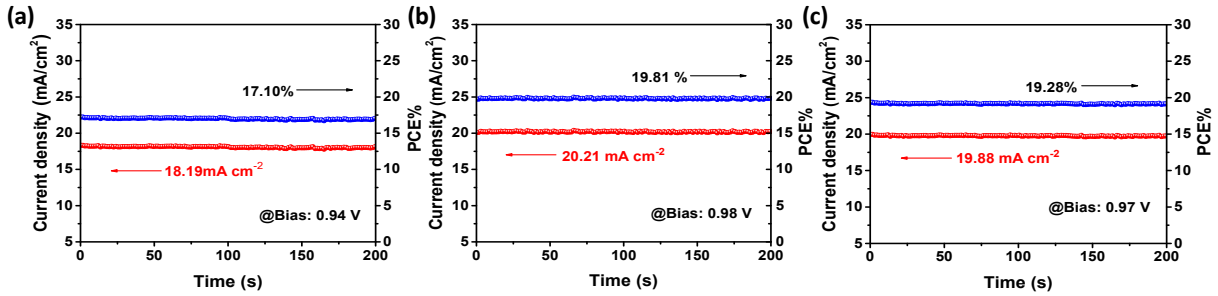

Figure S8. Steady-state photocurrent and PCE output of the PSCs based on (a) pure ZnO, (b) 2-TA and (c) 3-TA modified ZnO.

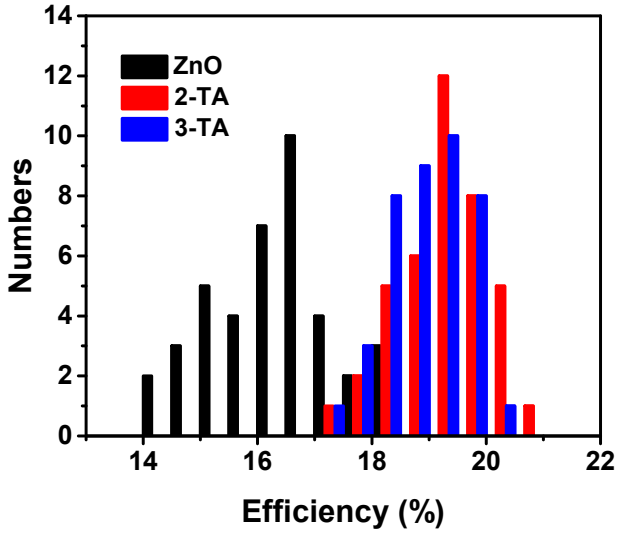

Figure S9. Histogram of PCEs measured for 40 PSCs based on pure ZnO, 2-TA and 3-TA modified ZnO, respectively.

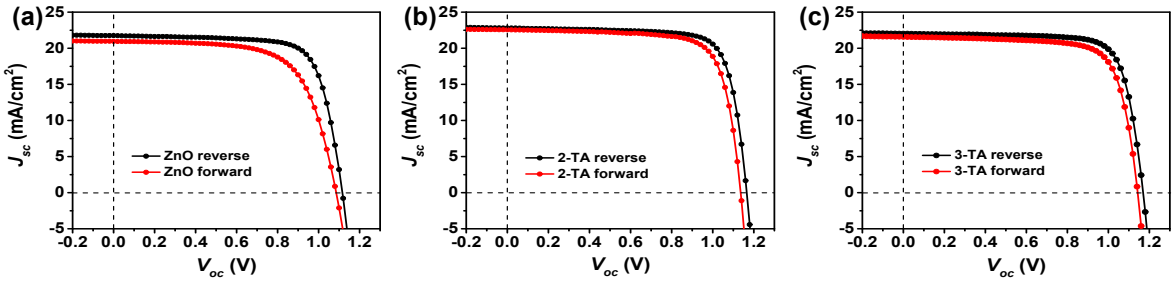

Figure S10. The *J-V* characteristics of devices a) without and with b) 2-TA and 3) 3-TA modification measured at 100 mWcm^{-2} AM 1.5G illumination under different scanning directions.

Table S2. The photovoltaic parameters of PSC devices without and with 2-TA and 3-TA modification obtained from Figure S10.

		V_{oc} / V	J_{sc} / mA cm^{-2}	FF / %	PCE / %	HI%
ZnO	reverse	1.12	21.7	74.5	18.1	16.0
	forward	1.09	21.0	66.6	15.2	

ZnO/2-TA	reverse	1.16	22.9	77.5	20.6	6.31
	forward	1.14	22.5	75.4	19.3	
ZnO/3-TA	reverse	1.17	22.1	77.3	20.0	7.50
	forward	1.14	21.6	75.1	18.5	

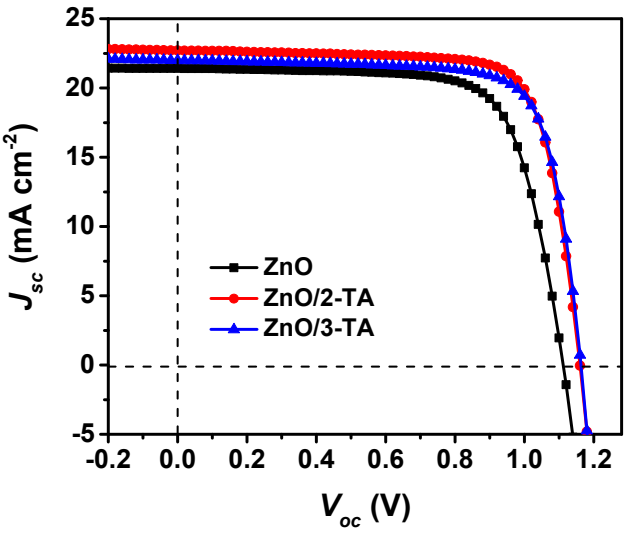

Figure S11. *J-V* characteristic of PSC devices based on the larger active area of 0.0945 cm^2.

Table S3. The photovoltaic parameters of PSCs obtained from Figure S11. Average and standard deviation values are obtained based on 10 cells and reported in brackets.

	V_{oc} / V	J_{sc} / mA cm^{-2}	FF / %	PCE / %
ZnO	1.11 (1.09 ± 0.02)	21.4 (20.2 ± 1.3)	72.8 (72.3 ± 2.0)	17.3 (16.0 ± 1.4)
ZnO/2-TA	1.16 (1.13 ± 0.02)	22.7 (21.5 ± 1.1)	76.7 (76.2 ± 1.5)	20.2 (18.6 ± 1.2)
ZnO/3-TA	1.16 (1.13 ± 0.02)	22.0 (21.0 ± 1.1)	76.4 (75.7 ± 1.6)	19.5 (18.1 ± 1.3)

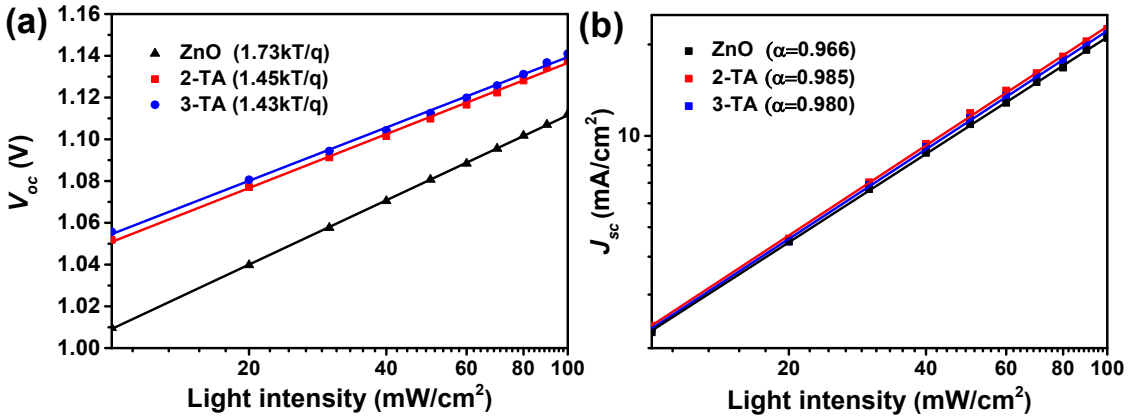

Figure S12. (a) V_{oc} and (b) J_{sc} dependence on light intensity for the PSC devices with and without TA modification from 10 to 100 mW/cm^2.

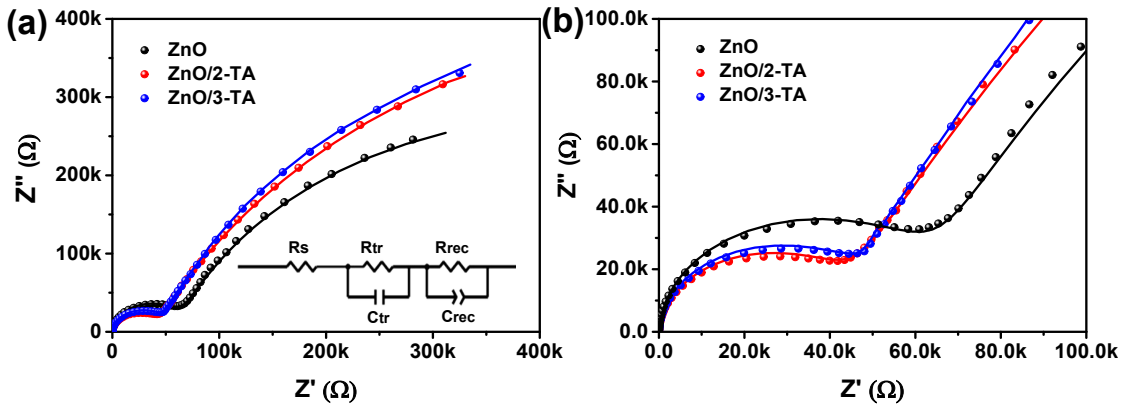

Figure S13. Electrochemical impedance spectroscopy (EIS) of the PSCs based on pristine and TA-modified ZnO. (a) Complete range and (b) zoom in the high-frequency region of the Nyquist plots, and inset is the equivalent circuit.

Table S4. Fitting parameters for EIS data acquired in the dark.

	ZnO	ZnO/2-TA	ZnO/3-TA
R_{tr} (kΩ)	59.1	40.0	44.6
R_{rec} (×10^5 Ω)	7.53	12.1	13.6

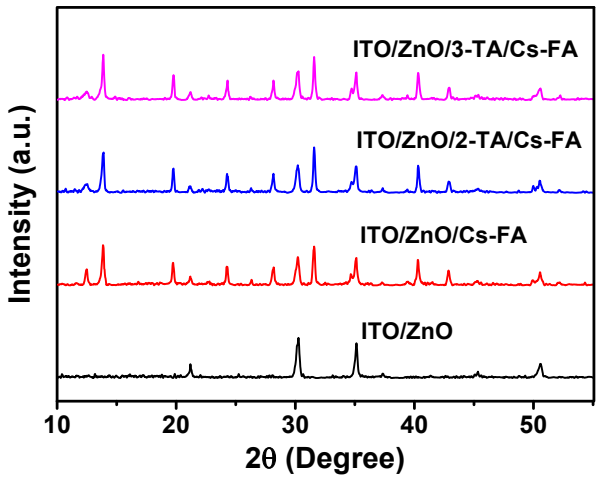

Figure S14. XRD patterns of Cs-FA films grown on the pristine and TA-modified ZnO ETLs with 110 °C annealing.

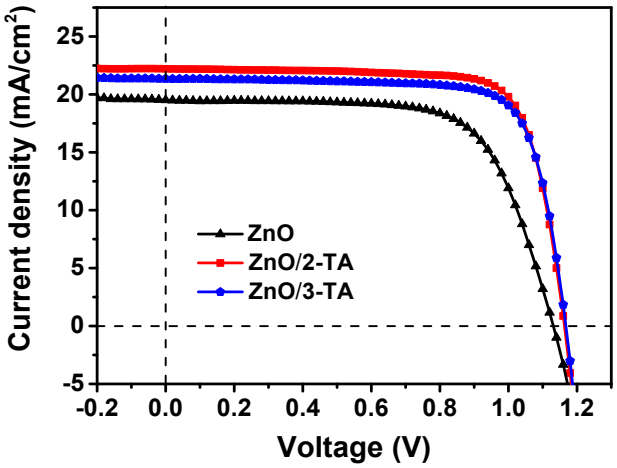

Figure S15. *J-V* curves of PSC device based on pristine and TA-modified ZnO, and the perovskite film was annealed at 110 °C.

Table S5. The photovoltaic parameters for PSCs based on ZnO ETLs obtained from Figure S14.

ETLs	V_{oc} / V	J_{sc} / mA cm^{-2}	FF / %	PCE / %
ZnO	1.13	19.5	68.3	15.0

ZnO/2-TA	1.16	22.2	77.2	19.9
ZnO/3-TA	1.17	21.4	76.8	19.2

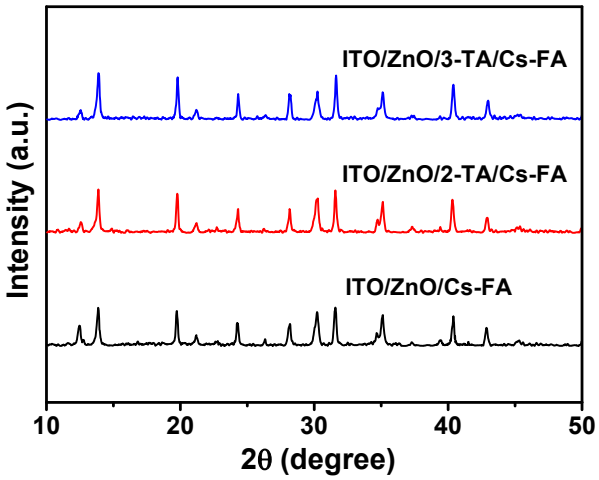

Figure S16. XRD patterns of perovskite films based on the pristine and TA-modified ZnO after storage in ambient condition for 330 h.

References

[1] Y. Li, Y. Zhao, Q. Chen, Y. (Michael) Yang, Y. Liu, Z. Hong, Z. Liu, Y.-T. Hsieh, L. Meng, Y. Li, Y. Yang, Multifunctional fullerene derivative for interface engineering in perovskite solar cells, *J. Am. Chem. Soc.* 2015, **137**, 15540-15547.